J. Anat. (1968), **103**, 1, pp. 49–63
With 14 *figures*
Printed in Great Britain

Fine structural study of the terminal effector plexus, neuromuscular and intermuscular relationships in the pulmonary artery

M. ANTHONY VERITY AND JOHN A. BEVAN

Departments of Pathology (Neuropathology) and Pharmacology, UCLA School of Medicine, Los Angeles, California 90024

Significant contributions towards a more detailed understanding of sympathetic nerve–smooth muscle transmission have come from *in vitro* studies of the innervated intestine and vas deferens and are the more valuable because of correlated ultrastructural observations (Richardson, 1958, 1962; Merrillees, Burnstock & Holman, 1963; Burnstock, Holman & Merrillees, 1962). The recent studies of Lever on the innervation of blood vessels have confirmed and extended many of the initial ultrastructural observations on the structure of the vascular wall (Moore & Ruska, 1957; Fawcett, 1959; Parker, 1958; Keech, 1960; Pease & Molinar, 1960; Pease & Paule, 1960; Karrer, 1961, Rhodin, 1962; Appenzeller, 1964). The significance of many of these morphologic observations is limited because correlative *in vitro* pharmacological and electrophysiological studies are lacking. The sympathetic nerve–pulmonary artery preparation (Bevan, 1962; Verity, Hughes & Bevan 1965) has allowed direct functional studies of vascular muscle reactivity following neural, direct muscle and drug induced stimulation.

The study investigates the nature of the innervation and the relationship between the terminal effector nerve plexus and the smooth muscle in the pulmonary artery–nerve preparation. Observations on intermuscular relationships, intermembrane distances and ultrastructural details of the sarcolemma are also presented.

MATERIALS AND METHODS

Young, mature rabbits, adult cats and kittens were used. The rabbits were stunned and bled; the cats were deeply anaesthetized with pentobarbitone administered intraperitoneally. The aortico-pulmonary complex was exposed through a bilateral longitudinal transcostal incision with removal of the sternal plate. The pericardium was opened and the pulmonary artery dissected free from the overriding aorta and surrounding fibro-adipose tissue.

The organization of the innervation apparatus of the pulmonary artery was visualized following intravital and supravital methylene-blue staining techniques (Verity *et al.* 1965). Fixation for electron microscopy was performed in two phases. Ice-cold phosphate buffered 3% glutaraldehyde was dripped upon the exposed pulmonary artery *in situ* for 3 min. The artery was rapidly removed, and multiple 1 mm sections of the pre-bifurcation area were cut and placed in 3% glutaraldehyde for 1 h at room temperature. Sections were washed in four changes of ice-cold phosphate buffer over a period of 2 h prior to post-fixation in 2% osmium tetroxide for 2 h at 2° C. The tissue was passed slowly through ascending grades of

ethanol at 2 °C prior to embedding in Epon 812. Sections were cut on an LKB Ultratome and stained with lead salts (Karnovsky, 1961) prior to examination in a Hitachi HU-11 electron microscope.

A quantitative analysis of the cellular architecture and extracellular space as revealed by electron microscopy was performed on prints enlarged to 11 × 14 in. at a final magnification of 15000–32000 after the method of Loud (1962). The linear grid (15 × 21 cm), containing 17 parallel lines 0·5 in. apart, was drawn upon matte acetate, 0·04 in. in thickness.

OBSERVATIONS

Light- and electron-microscopic observations on the prebirfucation area of the pulmonary artery in cats and rabbits revealed the typical organization of an elastic distributing artery characterized by concentric lamellae of elastin and smooth muscle. Ultrastructural details of the endothelium. the sub-endothelial layer or cytologic details of the adventitia differed only slightly from those of Buck (1958) in the rabbit; Pease & Paul (1960) and Keech (1960) in the rat.

Innervation

The pre-bifurcation region received a rich innervation from the right recurrent cardiac nerve. Post-ganglionic sympathetic fibres joined the nerve near its origin from the recurrent laryngeal or vagus and ramified at the bifurcation into antero-lateral and posterior branches to form the *primary adventitial plexus* (Verity *et al.* 1965). Schwann-cell nuclei stain palely with methylene blue and appear round or triangular, especially at regions of nerve-fibre confluence. The presence of Schwann cells, larger fibre size and the multiaxonal-organization limited to the adventitia readily distinguish this component of the nerve supply from the *terminal effector plexus* (Verity & Bevan, 1966), herein considered to represent the functional, principal catecholamine-storing site of the innervation apparatus. In methylene-blue preparations the terminal effector plexus consisted of a two-dimensional plexus of nerve bundles each containing 1–3 unmyelinated axons less than 1 μm in diameter and characterized by numerous round and fusiform swellings 0·2–0·5 μm in diameter. No Schwann nuclei were identified.

No specific relationship of the terminal effector plexus to the underlying smooth muscle, other than in its bidimensional organization at the adventitio-medial junction, was noted. Fibres from this plexus accompanied the superficially penetrating vasa vasora. Single, unmyelinated fibres from this perivasal plexus passed recurrently to adjacent portions of the terminal effector plexus. This morphological pattern of organization is diagrammatically summarized in Fig. 1.

Electron microscopy

Electron microscopy confirmed many details of the neural organization suggested by light microscopy. The ultrastructural morphology of the primary adventitial plexus revealed typical autonomic axonal bundles similar to those described by Hess (1955), Elfvin (1958), and Merrillees *et al.* (1963) and consisted of fascicles of 2–12 unmyelinated axons ensheathed by Schwann-cell cytoplasm. The axons were between 0·03 and 1·5 μm (mean = $0{\cdot}61 \pm 0{\cdot}04$) in diameter. The axoplasm was

moderately dense and contained mitochondria, occasional irregular, dense osmiophillic membrane-limited bodies resembling lysosomes, rare large granular vesicles, neurotubules and neurofilaments.

The terminal effector plexus of light microscopy is recognized electron microscopically as the probable functional site of transmitter storage and release. The identification of specialized axonal regions in the terminal effector plexus (Figs. 2–4) present an ultrastructural morphology highly suggestive of an adrenergic innervation (Verity & Bevan, 1966). These 'nerve terminal areas' (Lever, Ahmed & Irvine, 1965) were partially deficient of Schwann cytoplasm, contained numerous granular

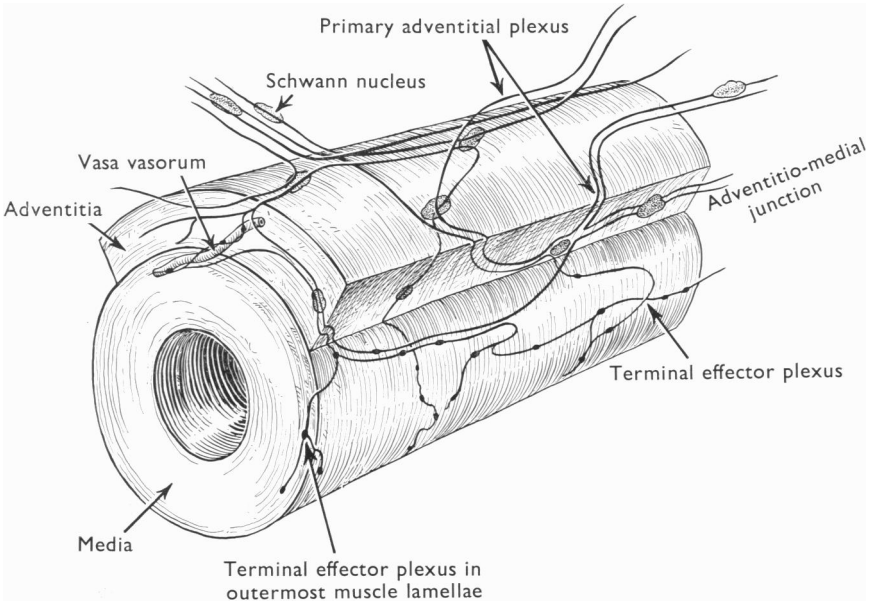

Fig. 1. Schematic representation of the neural organization of the pulmonary artery. Postganglionic sympathetic fibres of the recurrent cardiac nerve ramify in the adventitia to form the primary plexus. This plexus of unmyelinated nerves contains numerous Schwann-cell nuclei. The terminal effector plexus, essentially limited to the adventitio-medial junction, is the terminal continuation of the primary plexus. There is focal superficial penetration of the media in the perivasal plexus. The nodal specializations of axoplasm represent bare nerve terminal areas containing accumulations of granular vesicles.

vesicles, rare agranular microvesicles, large mitochondria typical of preterminal axoplasm and neurotubular profiles. The granular vesicles were of two varieties. The predominant form was similar to the type 1 granular vesicle of Grillo & Palay (1962). This vesicle was variable in shape and size, with a mean diameter of 975 Å (Fig. 5) whose osmiophilic dense core was surrounded by a distinct limiting membrane (Figs. 3, 4). Smaller granular vesicles $\sim$ 480 Å in diameter analogous to types 2 and 3 contained a small central osmiophilic core (Fig. 4).

Neurotubular profiles were commonly seen in the terminal effector plexus axoplasm. These neurotubules (present in greater numbers in the axoplasm of the primary adventitial plexus) had a cross-section diameter of $270{\cdot}1 \pm 1{\cdot}8$ Å ($n = 49$)

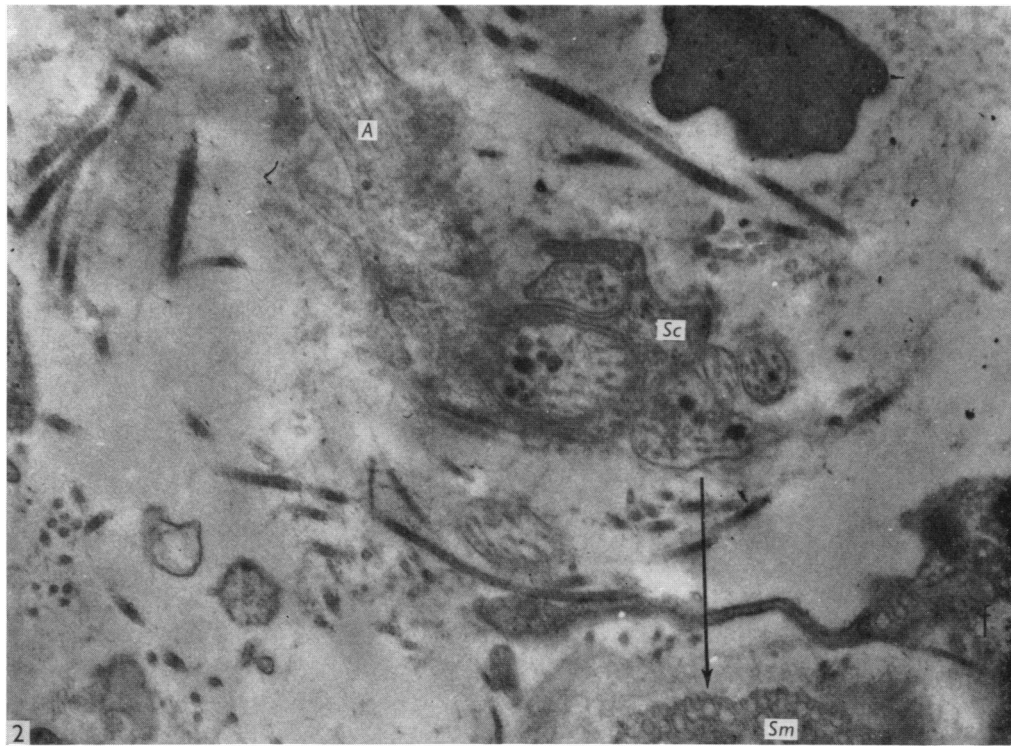
A
Sc
Sm
2

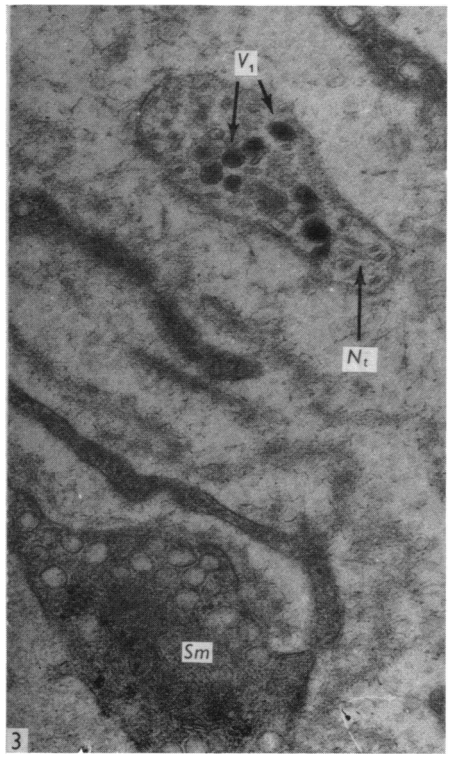
V_1
N_t
Sm
3

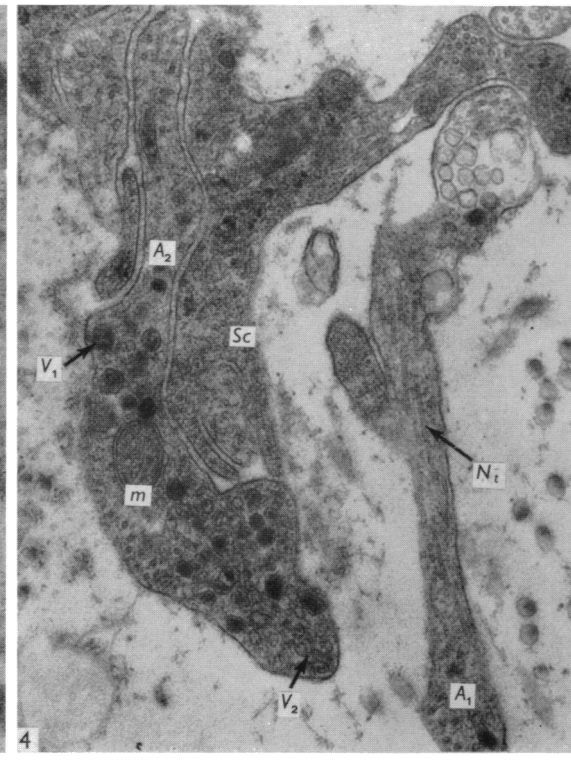
A_2
Sc
V_1
N_t
m
V_2
A_1
4

and 268·4 ± 3·2 Å (n = 54) when measured in transverse and longitudinal profiles respectively. The limiting osmiophilic membrane was 50–60 Å in width. The central light core often contained an inner denser filamentous structure, giving a 'target-ring' appearance (Figs. 4, 6, 6*a*), especially noticeable in the terminal portions of the plexus. Neurofilaments were not identified in the terminal effector plexus. The significant difference in size and regular shape of the transverse sections through neurotubules easily differentiated such structures from small granular vesicles.

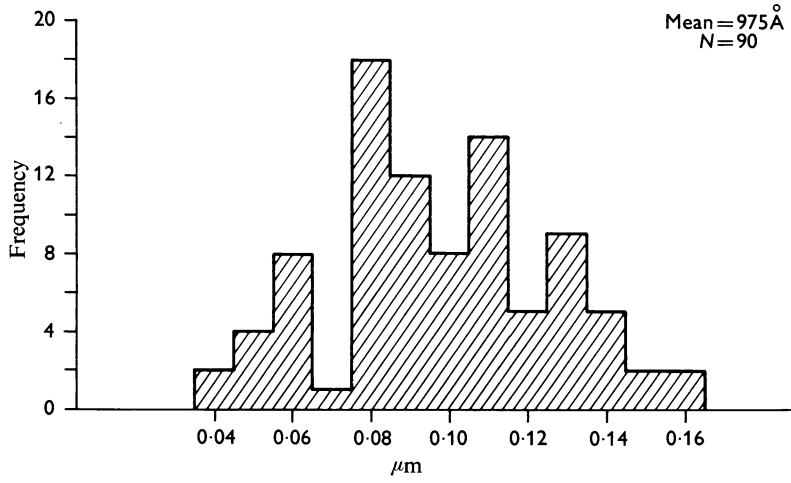

Fig. 5. Histogram of large granular vesicle size in bare nerve areas of the terminal effector plexus of the pulmonary artery. N = number of individual observations.

Attempts to obtain a mean value for the neuromuscular interval between the 'nerve terminal areas' of the axons (denuded of Schwann cytoplasm) and adjacent smooth-muscle plasmalemma revealed a mean value of 1·9 μm for the minimum neuromuscular interval and was obtained from measurements of thirty-five 'nerve terminal areas'. Of perhaps greater significance was the observation that no measured neuromuscular interval was less than 1000 Å; the narrowest interval being ~ 4000 Å (Verity & Bevan, 1966).

Fig. 2. Portion of terminal effector plexus in the adventitio-medial zone of the pulmonary artery. Four axons are partially enclosed by Schwann cytoplasm (*Sc*) but possess bare areas devoid of covering. Various granular vesicles, neurotubules, mitochondria and a few agranular vesicles are evident in the preterminal axoplasm. A fibroblast extension is interposed between the nerve terminal area and the distant (11000 Å) smooth muscle (*Sm*) sarcolemma. × 20000.

Fig. 3. Terminal axoplasm devoid of Schwann cell covering containing numerous large granular vesicles (V_1) surrounded by single membrane and few small granular profiles. Neurotubule segments (N_t) are conspicuous. × 25000.

Fig. 4. Granular vesicle-containing portion of terminal effector plexus, partially enclosed by Schwann cytoplasm (*Sc*). Large (V_1) and small (V_2) vesicles are seen. Long profiles of neurotubules (N_t) are present in an adjacent unmyelinated axon (A_1) and transversely sectioned neurotubules are identified in axon (A_2). × 25000.

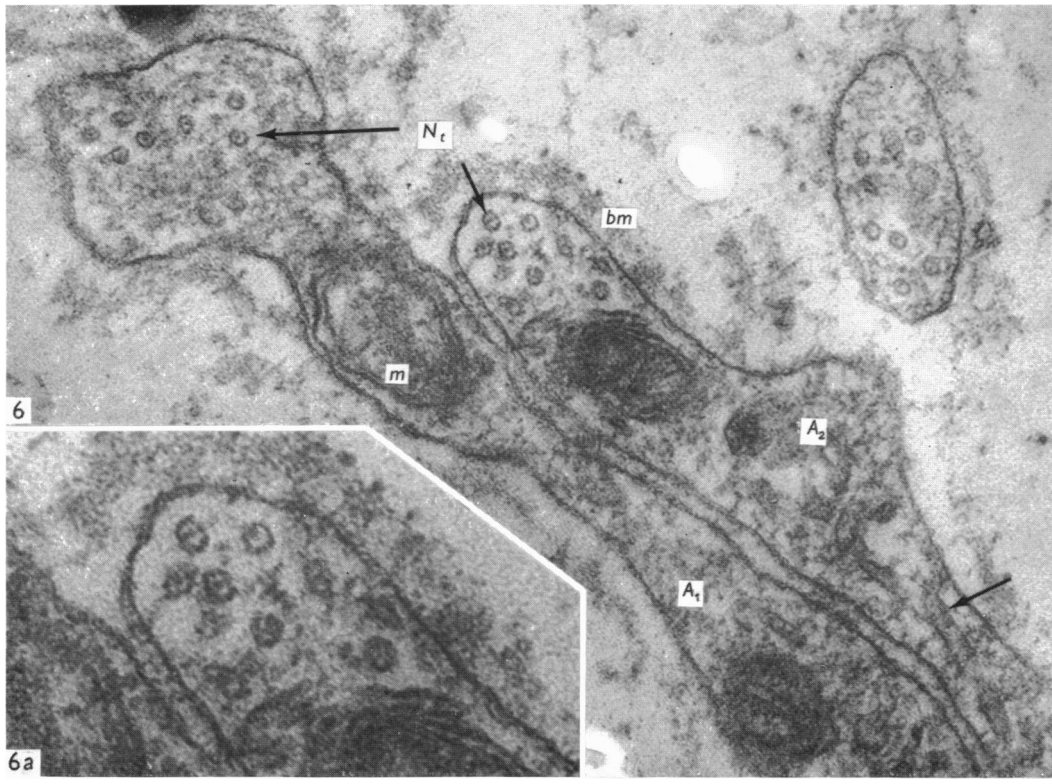
N_t
bm
m
A_2
A_1
6
6a

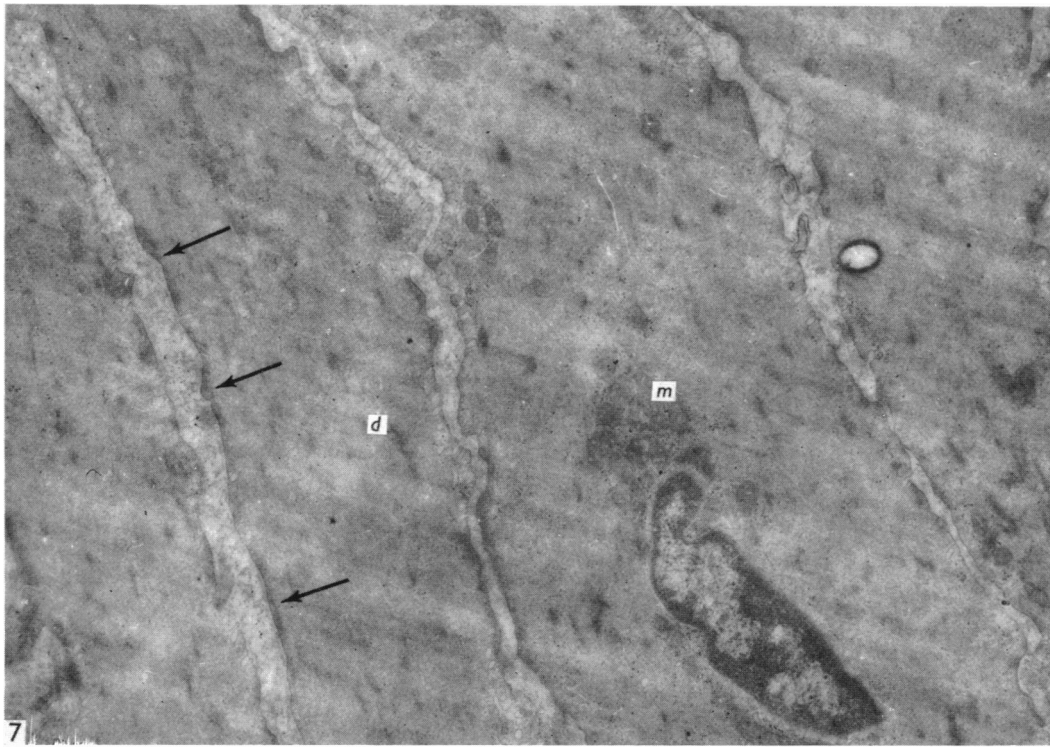
m
d
7

SMOOTH MUSCLE

General organization

The smooth muscle of the pulmonary artery was irregularly disposed, and loosely aggregated in the adventitio-medial zone, but assumed a lamellar orientation in the deeper layers of the media (Fig. 7). Collagen fibrils and microfibrillar material loosely surrounded individual muscle cells except in regions of apposition with elastic lamellae (Fig. 8) and areas of close muscular juxtaposition.

The sarcoplasm contained polar orientated mitochondria, specialized Golgi zones, centrioles, and an indented nucleus. The endoplasmic reticulum was concentrated in the perinuclear zone where poorly developed smooth and rough-surfaced components were visualized. Ribonucleoprotein particles and glycogen was scattered throughout the cytoplasm. The myofilaments were arranged in loose bundles usually running parallel to an adjacent portion of the cell membrane. Elongated, dense bars were seen in the sarcoplasm (Figs. 7, 9), arranged parallel to the myofilaments (Merrillees *et al.* 1963; Pease & Molinar, 1960).

Sarcoplasmic membrane and sub-sarcoplasmic organization

Individual smooth muscle cells were limited by a trilaminar plasmalemma, ~ 80 Å in width, easily visualized in the cytoplasmic extrusions and micropinocytic vacuolations. There was a clear space between the plasmalemma and basement membrane. The latter varied in thickness from 300 to 700 Å and often appeared adherent to the plasmalemma by filamentous material. The basement membrane was especially prominent over the dense areas of plasmalemma but was attenuated over regions of micropinocytic vacuolation (Figs. 9, 13).

A characteristic feature of the plasmalemma of pulmonary artery smooth muscle was the extensive micropinocytic vacuolation previously observed in smooth muscle (Moore & Ruska, 1957; Lever, Ahmed & Irvine, 1965). Occurring especially in the adventitio-medial smooth muscle lamellae, the vacuolation occurred on the adventitial and intimal aspects of the membrane in characteristic segments 0·2–1 μm in length. The vacuoles were often flask-shaped with maximum and minimum diameters of ~ 1200 Å and ~ 850 Å respectively. They were usually arranged in a single layer, but did not contain basement-membrane material and were associated rarely with segments of the dilated subsurface endoplasmic reticulum.

Extracellular and intermembrane space

An electron-microscopic determination of the muscularis extracellular space was made by a linear sampling procedure on multiple prints (Loud, 1962). Expressions

Fig. 6. Two axons (A_1, A_2) of the terminal effector plexus devoid of Schwann-cell covering with granular vesicular material, prominent neurotubular profiles (N_t and arrow) and mitochondria in the axoplasm. The surrounding basement membrane (*bm*) is tenuous. × 80000. Insert (Fig. 6*a*) shows the prominent central filamentous core of the neurotubules and the trilaminar structure of the axolemma. × 180000.

Fig. 7. Longitudinal sections of four smooth muscles in the pulmonary artery muscularis. The sarcolemma contains alternating areas of pinocytic vacuolation and dense zones. Fusiform densities (*d*) oriented to the long axis are present throughout the sarcoplasm. The mitochondria assume a polar position beside the nucleus. × 16000.

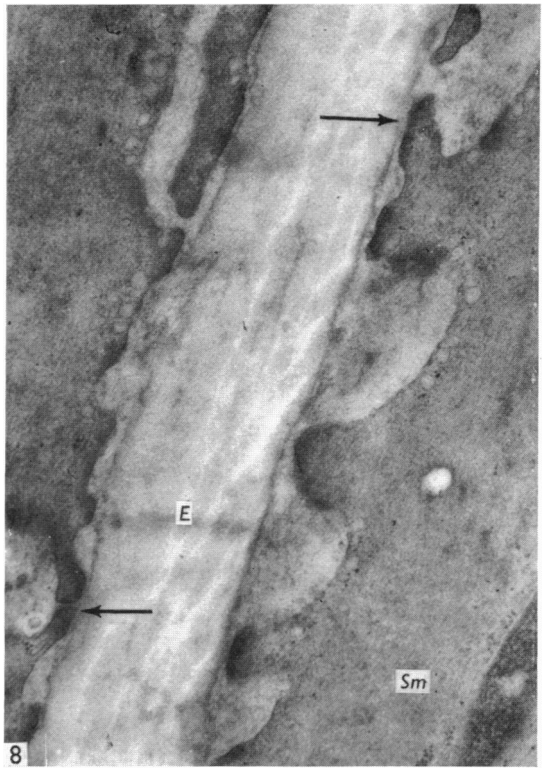

8

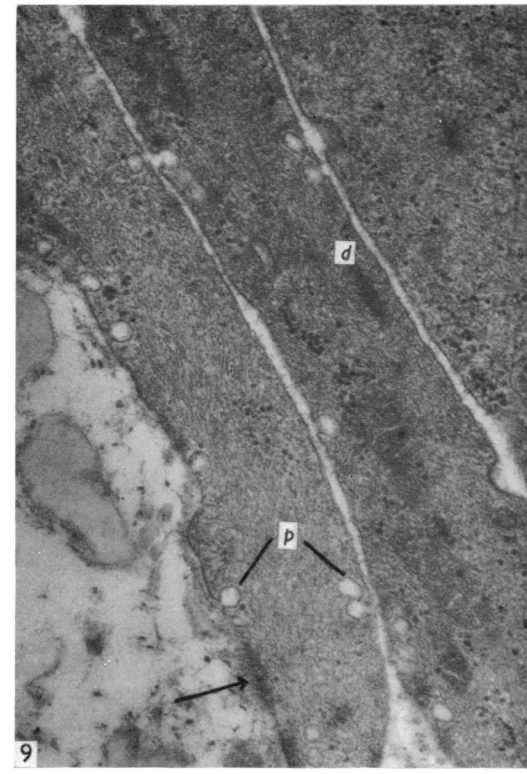

9

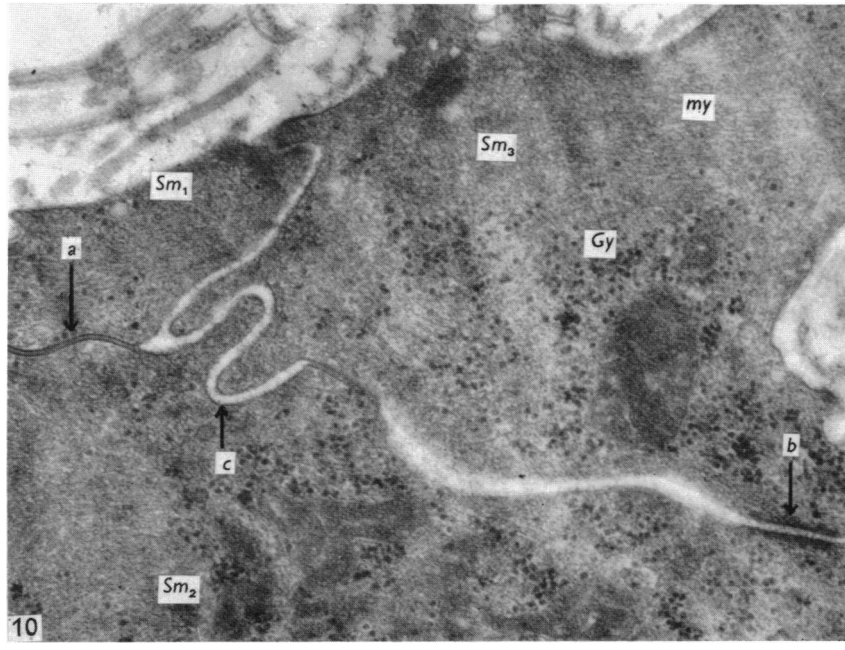

10

of the extracellular space as a percentage of the total volume of the muscularis were obtained, as two-dimensional measurements can be extended to the fraction of tissue volume occupied by the cellular and non-cellular compartments. The smooth muscle accounted for 54·5 ± 5·8 (S.E.M.) %, while the extracellular compartment from these measurements was 32·3 % (Table 1).

Table 1. *Quantitative estimate of percentage (mean ± S.E.M.) smooth-muscle content and extracellular space in pulmonary artery muscularis as determined from electron micrographs (after Loud, 1962)*

No. of prints	Total print area (*a*)	Smooth muscle (*b*)	Elastin (*c*)	Collagen, microfibrillar material, basement membrane (*d*)	Mean extramuscular space (*a*−*b*)	Extracellular space *a*−(*b*+*c*+*d*)
14	100	54·5 ± 5·8	9·0 ± 2·6	4·3 ± 2·0	45·5	32·2

Regions of close smooth-muscle membrane juxtaposition were represented by tongue-like sarcoplasmic invaginations ('peg and socket') of one smooth muscle cell with an adjacent cell (Fig. 12). Areas of closer junctional apposition between smooth muscle cells were *very rare* but represented either by nexus-like planar contacts (Figs. 10, 11) or desmosomes (Fig. 10). The nexus-like contact was a quintuplet structure, the central osmiophilic lamina being formed by coalescence of merging outer portions of the basement membrane. This probably represents the configuration in osmium-fixed tissue corresponding to the nexus seen in permanganate fixation (Lane & Rhodin, 1964). The desmosomal junction was wider, contained dense homogeneous interfacial material and increased osmiophilia of the immediate subplasmalemmal sarcoplasm. A measure of smooth muscle interplasmalemmal distance was provided from intermembrane distances of adjacent cells in which both nuclei were visible. An estimate of the minimum intermembrane distance on selected micrographs of the muscularis was made by subjectively placing a grid perpendicular to the axis of the intermembrane space. Measurements were made at

Fig. 8. Part of pulmonary artery media showing lateral margins of two smooth muscle cells separated by homogeneous elastic tissue. The smooth muscle (*Sm*) runs obliquely and is focally attached to the elastin lamellae by desmosome-like dense zones (arrows). × 20000.

Fig. 9. Portion of media reveals the variable size of the micropinocytic vacuolations (*p*) and basement membrane prominance adjacent to sarcolemmal dense zones (arrow). The myofibrils are more easily seen in our dichromate fixed material. The myofibrils pass through the sarcoplasmic fusiform densities (*d*) without interruption. × 24000.

Fig. 10. Portions of three smooth-muscle cells of the pulmonary artery media (Sm_{1-3}) showing two types of *rare* sarcolemmal junctional complexes (*a*, *b*) and less rare cell-to-cell invaginations (*c*). Complex (*a*) is a planar contact. The desmosomal complex (*b*) is wider, with thickening and increased density of the interfacial material (basement membrane). The immediate subplasmalemmal cytoplasm has the approximate dimensions of a dense bar, but also shows a lamellae substructure. A 'lattice' orientation of the myofilaments (*my*) is seen in the smooth muscle (Sm_3). Numerous mitochondria and glycogen aggregates (*Gy*) are noted in the sarcoplasm. × 25000.

10 mm intervals along the grid. The mean intermembrane distance was calculated as $6{\cdot}06 \times 10^3$ Å (Fig. 14); 3·5 % of the measurements were less than 500 Å, and 0·9 % of the measurements were 200 Å or less.

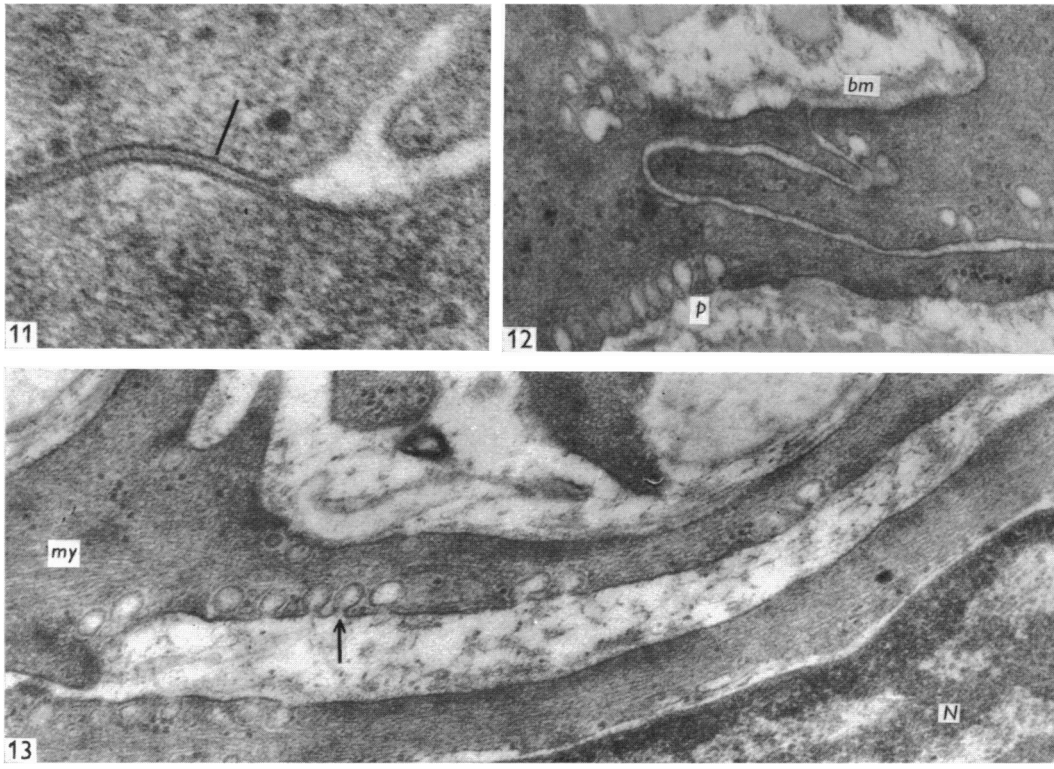

Fig. 11. Detail of nexus-like planar contact shown in Fig. 8. The quintuple layered membrane junction is ~ 120 Å in width. × 150000.

Fig. 12. A typical 'peg and socket' junctional complex. The adjacent basement membrane (*bm*) is also separated from the plasmalemma by a well defined clear space containing delicate filamentous strands. × 24000.

Fig. 13. The submembranous, longitudinal orientation of the myofilaments (*my*) is interrupted by micropinocytic vacuolation. The vacuoles are flask-shaped, often open to the extracellular space and only rarely in contact with dilated portions of the endoplasmic reticulum. Basement membrane is very attenuated or absent adjacent to regions of vacuolation. × 35000.

DISCUSSION

Numerous reports have described various neuromuscular relationships, including three-dimensional interrelations, in smooth muscle of different tissues and animals. Significant to this discussion are those observations pertaining to the intercellular and neuromuscular relationships in vascular smooth muscle. Fluorescence studies (Norberg & Hamberger, 1964; Ehinger & Sporrong, 1966) have revealed a typical, nodose, adrenergic ground plexus directly superimposed upon the smooth muscle of the vasculature. Ultra-structural studies of neuromuscular relationships (Lever &

Esterhuizen, 1961; Lever, Ahmed & Irvine, 1965; Appenzeller, 1964; Lever, Graham, Irvine & Chick, 1965; Zelander, Ekholm & Edlund, 1962; Samarasinghe, 1963; Simpson & Devine, 1966) have revealed vesiculated axons in the adventitia partially covered by Schwann-cell cytoplasm. The neuromuscular organization of the pulmonary artery, diagrammatically summarized in Fig. 1, demonstrated many features of similarity to the neural organization of arterioles and muscular arteries. A significant difference was noted in the vesicular content of the axoplasmic expansions ('nerve terminal area') of the terminal effector plexus. The plurivesicular material contained a

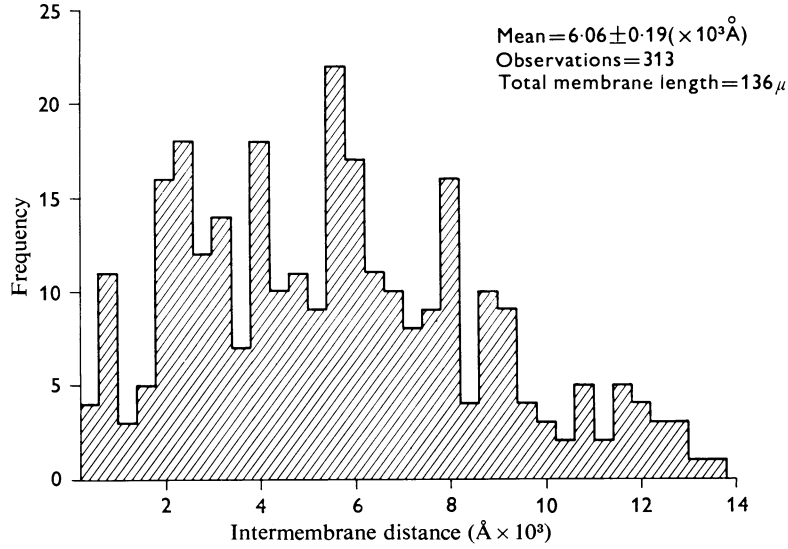

Fig. 14. Frequency distribution of intermembrane distance of the smooth-muscle sarcolemma in the media of the pulmonary artery of the rabbit. The total membrane length of 136 μm was obtained from thirty-two prints; mean print magnification, × 18000.

predominant population of large granular forms, ~ 975 Å in diameter. Plurivesicular adrenergic nerve endings characterized by large type 1 vesicles have been found in the pineal gland, periarterial branches of the splenic nerve (de Robertis & de Iraldi, 1961), and anterior hypothalamus of the rat (de Iraldi, Duggan & de Robertis, 1963). The proportion of large type 1 to smaller types 2, and 3 granules varies from tissue to tissue, approximately 10% being type 1 in pancreatic arterioles, contrasted to 90% in the anterior hypothalamus. Numerous agranular vesicles are frequent in most tissues. Moreover, type I vesicles have been shown to occur in the axons of the guinea-pig vas deferens (Merrillees *et al.* 1963), rabbit eye sphincter (Richardson, 1962) and preganglionic terminals supplying adrenal medullary cells (Coupland, 1965). They are not found in the rabbit iris dilator muscle or rat vas deferens.

Evidence for the association of granular vesicles with catecholamines appears very strong. The radioautographic localization of tritiated noradrenaline with granular vesicles in the terminal parts of sympathetic axons in the pineal gland (Wolfe, Potter, Richardson & Axelrod, 1962) and rat heart (Wolfe & Potter, 1963)

has been demonstrated. Furthermore, the usefulness and specificity of primary glutaraldehyde fixation in the selective production of electron density in noradrenaline containing vesicles has been demonstrated (Zelander *et al.* 1962; Bloom & Barrnett, 1966). Pharmacological evidence in this respect has come from studies with reserpine and α-methyl metatyrosine which are known to selectively deplete noradrenaline stores. These agents induced a degranulation of the *small* granular vesicles (Bondareff, 1965; Bloom & Barrnett, 1966; Hökfelt, 1966), but no recognizable loss of electron-dense material was noted from the *large* granules, ~ 800–1200 Å. Although the anterior hypothalamus has a high concentration of noradrenaline (Vogt, 1954; Carlsson, Falck & Hillarp, 1962) the granular vesicles are predominantly of the large size (type I). Moreover, a close correlation between noradrenaline content and numbers of granulated vesicles has been demonstrated in this tissue (Ishii, Shimizu, Matsuoka & Imaizumi, 1965; de Robertis, de Iraldi, de Arnaiz & Zieher, 1965). These observations indicate the noradrenaline nature of the small granular vesicles and presumed noradrenaline localization in large vesicles but they cast no light on the nature of the drug resistance of the large, type I vesicles.

The low innervation density of the pulmonary artery contrasts strongly with that of the ductus deferens, iris and ciliary body, where several neuroeffector 'contacts' are made over a few microns of muscularis (Merrillees *et al.* 1963; Richardson, 1962). The minimum neuromuscular interval in the pulmonary artery is ~ 4000 Å. Moreover, the two-dimensional organization or the terminal effector innervation, limited to the adventitio-medial junction, precludes innervation to more than three-quarters of the muscularis. Electrophysiologic studies have indicated that a propagated action potential occurs between most smooth-muscle cells (Prosser, Burnstock & Kahn, 1960). However, Sperelakis & Tarr (1965) reported a weak interaction between intestinal muscle cells and concluded that no substantial transfer of excitation occurred. Pulmonary artery smooth muscle is electrically quiescent (Su, Bevan & Ursillo, 1964) to sympathetic nerve stimulation and norepinephrine, thus negating electrogenic spread of excitation and strongly suggesting that the initiation of muscular contraction is due to non-electrogenic membrane events following transmitter diffusion. Of interest in this connexion is the value of 32% obtained as an index of the extracellular compartment. This agrees favourably with values of 39% for the carotid artery (Prosser *et al.* 1960) and 38% for the inulin space in ileal smooth muscle (Weiss, 1966), but is in sharp contrast to values of 8% for vas deferens (Lane & Rhodin, 1964) and 18% for retractor penis (Prosser *et al.* 1960), tissues characterized by many neuroeffector contacts (see below). The few loci of membrane fusion (see Fig. 11) in pulmonary artery muscularis (as visualized in osmium fixed material) would not be an impediment to transmitter diffusion. Such regions are very similar to those contact points visualized between intestinal muscle cells by Lane & Rhodin (1964, see their Fig. 8). Intermembrane distance, over a total membrane length of 138 μm, showed less than 3·5% < 500 Å distant, with a mean intermembrane distance of $6{\cdot}06 \times 10^3$ Å. The mean intercellular distance in tenia coli is $0{\cdot}69 \times 10^3$ Å with multiple wide spacings, and ~ $1{\cdot}0 \times 10^4$ Å, in the carotid artery (Prosser *et al.* 1960).

Bevan & Verity (1996) found a long latency (1·06 ± 0·04 sec) between the commencement of repetitive nerve stimulation and the beginning of a contractile response in the

pulmonary artery–nerve preparation. The shortest observed distance between a 'nerve terminal' area and the plasma membrane of vascular smooth muscle was 0·4 μm with a mean of 1·9 μm. This large neuromuscular interval is in marked contrast to that found in the vas deferens, where 1 % of the smooth muscle cells are in immediate contact, i.e. separated by $< 0{\cdot}02$ μm (Merrillees, Burnstock & Holman, 1963). In a provisional analysis of the genesis of the delay in vascular smooth muscle attention has been drawn to the phenomena occurring *after* release of the transmitter from its storage site and completion of its receptor interaction. Pugsley, (quoted by Merrillees, Burnstock & Holman, 1963) calculated that the time taken for a quantum of noradrenaline to diffuse over a distance of 1 μm is considerably less than the time required for the junctional potentials in the vas deferens to reach maximum amplitude. In this tissue the latency between stimulation of hypogastric nerve and initiation of junctional potentials is 20–100 ms (Burnstock & Holman, 1961). This time, which includes a ganglionic delay, represents only 10 % of the latency in the pulmonary artery preparation. It is thus unlikely that extracellular diffusion alone can account for the long latency. The fact that only adrenergic blocking agents, e.g. yohimbine and SY-14, significantly prolonged the latency indicates the importance of the effective concentration of transmitter at the receptor site, presumed to be adrenergic. Electron microscopy reveals a minimum amount of microfibrillary material and collagen in the diffusional space, and an ill-defined basement membrane. This mucopolysaccharide barrier may significantly contribute to the nerve–muscle delay, but other rate limiting steps with high temperature coefficients cannot be excluded.

SUMMARY

An electron-microscope study of the innervation and intermuscular relationships of pulmonary artery smooth muscle in cats and rabbits has been performed. Previous observations of light microscopy suggesting the presence of a primary adventitial nerve plexus and a terminal plexus limited to the adventitio-medial zone were confirmed. The primary adventitial plexus consisted of fascicles of unmyelinated axons surrounded by Schwann cytoplasm. The axons contained prominent neurotubules and neurofilaments. The terminal effector plexus contained specialized nerve-terminal areas partially deficient in Schwann cytoplasmic covering. These areas contained large mitochondria, neurotubular profiles, granular and rare agranular vesicles. The predominant membrane limited granular vesicle (type 1) was variable in shape and size, and contained a dense, granular core. Types 2 and 3 granular vesicles, $\sim$ 480 Å in diameter, were identified. The mean 'neuromuscular' distance between the nerve terminal areas and adjacent smooth muscle plasmalemma was 1·9 μm with a minimum interval of 4000 Å. There was extensive micropinocytic vacuolation of the smooth-muscle plasmalemma, especially in the outer lamellae. Membrane-to-membrane specializations were rare but represented by peg and socket invaginations, planar contacts and desmosomes. These observations are correlated with recent pharmacological data and indicate that smooth-muscle activation is dependent upon transmitter diffusion from specialized axon areas.

This work was supported in part by grants from the United States Public Health Service, HE-08359, and Multiple Sclerosis Society, Grant no. 385.

The authors wish to express their indebtedness to Messrs R. J. Ostrom and T. Dohl for excellent technical assistance.

REFERENCES

APPENZELLER, O. (1964). Electron microscopic study of the innervation of the auricular artery of the rat. *J. Anat.* **98**, 87–91.

BEVAN, J. A. (1962). Some characteristics of the isolated sympathetic nerve–pulmonary artery preparation of the rabbit. *J. Pharmacol.* **137**, 213–218.

BEVAN, J. A. & VERITY, M. A. (1966). Postganglionic sympathetic delay in vascular smooth muscle. *J. Pharmacol.* **152**, 221–230.

BLOOM, F. E. & BARRNETT, R. J. (1966). Fine structural localization of noradrenaline in vesicles of autonomic nerve endings. *Nature, Lond.* **210**, 599–601.

BONDAREFF, W. (1965). Submicroscopic morphology of granular vesicles in sympathetic nerves of rat pineal body. *Zellforsch. Z.* **67**, 211–218.

BUCK, R. C. (1958). The fine structure of the aortic endothelial lesions in experimental cholesterol atherosclerosis of rabbits. *Am. J. Path.* **34**, 897–909.

BURNSTOCK, G. & HOLMAN, M. E. (1961). The transmission of excitation from autonomic nerve to smooth muscle. *J. Physiol., Lond.* **155**, 115–133.

CAESAR, R., EDWARDS, G. A. & RUSKA, H. (1957). Architecture and nerve supply of mammalian smooth muscle tissues. *J. biophys. biochem. Cytol.* **3**, 867–877.

CARLSSON, A., FALCK, B. & HILLARP, N.-A. (1962). Cellular localization of brain monoamines. *Acta physiol. Scand.* **56**, Suppl. 196.

COUPLAND, R. E. (1965). Electron microscopic observations on the structure of the rat adrenal medulla. *J. Anat.* **99**, 255–272.

DE IRALDI, A. P., DUGGAN, H. F. & DE ROBERTIS, E. (1963). Adrenergic synaptic vesicles in the anterior hypothalamus of the rat. *Anat. Rec.* **145**, 521–531.

DE ROBERTIS, E. & DE IRALDI, A. P. (1961). A plurivesicular component in adrenergic nerve endings. *Anat. Rec.* **139**, 299.

DE ROBERTIS, E., DE IRALDI, A. P., DE L. ARNAIZ, G. R. & ZIEHER, L. M. (1965). Synaptic vesicles from the rat hypothalamus. Isolation and norepinephrine content. *Life Sci.* **4**, 193–201.

EHINGER, B. & SPORRONG, B. (1966). Symposium on Electrical Activity and Innervation of Blood vessels. *Proc. 4th Europ. Microcirculatory Conf.*, Oxford.

ELFVIN, L.-G. (1958). The ultrastructure of unmyelinated fibers in the splenic nerve of the cat. *J. Ultrastruct. Res.* **1**, 428–454.

FAWCETT, D. W. (1959). In *Microcirculation* (Ed. S. R. M. Reynolds and B. W. Zweifach), pp. 1–27. University of Illinois Press.

GRILLO, M. & PALAY, S. L. (1962). In *Electron Microscopy* (Ed. S. S. Breese, Jr.), U-1, New York: Academic Press.

HESS, A. (1955). The fine structure and morphological organization of non-myelinated nerve fibres. *Proc. R. Soc.* B, **144** 496–506.

HÖKFELT, T. (1966). The effect of reserpine on the intra-neuronal vesicles of the rat vas deferens. *Experientia* **22**, 56.

ISHII, S., SHIMIZU, N., MATSUOKA, M. & IMAIZUMI, R. (1965). Correlation between catecholamine content and numbers of granulated vesicles in rabbit hypothalamus. *Biochem. Pharmacol.* **14**, 183.

KARNOVSKY, M. J. (1961). Simple methods for 'staining with lead' at high pH electron microscopy. *J. biophys. biochem. Cytol.* **11**, 729–732.

KARRER, H. E. (1961). An electron microscope study of the aorta in young and in aging mice. *J. Ultrastruct. Res.* **5**, 1–27.

KEECH, M. K. (1960). Electron microscope study of the normal rat aorta. *J. biophys. biochem. Cytol.* **7**, 533–538.

LANE, B. P. & RHODIN, J. A. G. (1964). Cellular interrelationships and electrical activity in two types of smooth muscle. *J. Ultrastruct. Res.* **10**, 470–488.

LEVER, J. D. & ESTERHUIZEN, A. C. (1961). Fine structure of the arteriolar nerves in the guinea pig pancreas. *Nature, Lond.* **192**, 566–567.

LEVER, J. D., AHMED, M. & IRVINE, G. (1965). Neuromuscular and intercellular relationships in the coronary arterioles. A morphological and quantitative study by light and electron microscopy. *J. Anat.* **99**, 829–840.

LEVER, J. D., GRAHAM, J. D. P., IRVINE, G. & CHICK, W. J. (1965). The vesiculated axons in relation to arteriolar smooth muscle in the pancreas. A fine structural and quantitative study. *J. Anat.* **99**, 299–313.

LOUD, A. V. (1962). A method for the quantitative estimation of cytoplasmic structures. *J. Cell Biol.* **15**, 481–487.

MERRILLEES, N. C. R., BURNSTOCK, G. & HOLMAN, M. E. (1963). Correlation of fine structure and physiology of the innervation of smooth muscle in the guinea pig vas deferens. *J. Cell Biol.* **19**, 529–550.

MOORE, D. H. & RUSKA, H. (1957). The fine structure of capillaries and small arteries. *J. biophys. biochem. Cytol.* **3**, 457–462.

NORBERG, K.-A. & HAMBERGER, B. (1964). The sympathetic adrenergic neuron. *Acta physiol. Scand.* **63**, Suppl. 238.

PARKER, F. (1958). An electron microscope study of coronary arteries. *Am. J. Anat.* **103**, 247–273.

PEASE, D. C. & MOLINAR, S. (1960). Electron microscopy of muscular arteries; pial vessels of the cat and monkey. *J. Ultrastruct. Res.* **3**, 447–468.

PEASE, D. C. & PAULE, W. J. (1960). Electron microscopy of elastic arteries; the thoracic aorta of the rat. *J. Ultrastruct. Res.* **3**, 469–483.

PROSSER, C. L., BURNSTOCK, G. & KAHN, J. (1960). Conduction in smooth muscle; comparative structural properties. *Am. J. Physiol.* **199**, 545–559.

RHODIN, J. A. G. (1962). Fine structure of vascular walls in mammals with special reference to smooth muscle component. *Physiol. Rev.*, **42**, Suppl. 5, 48–87

RICHARDSON, K. C. (1958). Electronmicroscopic observations on Auerbach's plexus in the rabbit, with special reference to the problem of smooth muscle innervation. *Am. J. Anat.* **103**, 99–103.

RICHARDSON, K. C. (1962). The fine structure of autonomic rabbit iris with special reference to the identification of adrenergic and cholinergic nerves and nerve endings in its intrinsic muscles. *Am. J. Anat.* **114**, 173–184.

SAMARASINGHE, D. D. (1963). An electron microscopic study of the arteries to the brain of the rat with special reference to the accompanying nerve fibres. *J. Anat.* **97**, 311.

SIMPSON, F. O. & DEVINE, C. E. (1966). The fine structure of autonomic neuromuscular contacts in arterioles of sheep renal cortex. *J. Anat.* **100**,127–137.

SPERELAKIS, N. & TARR, M. (1965). Weak electronic interaction between neighboring visceral smooth muscle cells. *Am. J. Physiol.* **208**, 737–747.

SU, C., BEVAN, J. A. & URSILLO, R. C. (1964). Electrical quiescence of pulmonary artery smooth muscle during sympathomimetic stimulation. *Circulation Res.* **15**, 20–57.

VERITY, M. A., HUGHES, T. & BEVAN, J. A. (1965). Innervation of the pulmonary artery bifurcation of the cat. *Am. J. Anat.* **116**, 75–90.

VERITY, M. A. & BEVAN, J. A. (1966). Morphopharmacologic studies of the innervation of the pulmonary artery. In Symposium on 'Electrical Activity and Innervation of Blood Vessels.' *Proc. 4th Europ. Microcirculatory Conf.* Oxford.

VERITY, M. A. & BEVAN, J. A. (1966). Plurivesicular nerve endings in the pulmonary artery. *Nature, Lond.* **211**, 537–538.

VOGT, M. (1954). The concentration of sympathin in different parts of the central nervous system under normal conditions and after the administration of drugs. *J. Physiol., Lond.* **123**, 451–481.

WEISS, G. B. (1966). Homogeneity of extracellular space measurement in smooth muscle. *Am. J. Physiol.* **210**, 771–776.

WOLFE, D. E., POTTER, L. T., RICHARDSON, K. C. & AXELROD, J. (1962). Localizing tritiated norepinephrine in sympathetic axons by electron microscopic autoradiography. *Science, N.Y.* **138**, 440–442.

WOLFE, D. E. & POTTER, L. T. (1963). Localization of norepinephrine in the atrial myocardium. *Anat. Rec.* **145**, 301.

ZELANDER, T., EKHOLM, R. & EDLUND, Y. (1962). The ultrastructural organization of the rat exocrine pancreas. III. Intralobular vessels and nerves. *J. Ultrastruct. Res.* **7**, 84–101.